

Mixed Kaon Condensation in CFL Matter

Andrei Kryjevski ^{*} and Travis Norsen [†]

Dept. of Physics and Institute for Nuclear Theory, University of Washington, Seattle, WA 98195

(November 4, 2018)

Abstract

Previous work on high-density QCD suggests that the ground state configuration in the presence of a non-zero neutrino chemical potential consists of CFL matter plus a homogeneous condensate of neutral and positive kaons. We consider here the stability of this homogeneous configuration toward the production of a charge-separated mixed phase, and find that the system is indeed stable against the production of such a heterogenous configuration. We identify the critical value of the fine structure constant which would allow for phase separation. We also derive dispersion relations for the low-lying excitations above the kaon-condensed ground state and discuss their possible phenomenological implications.

I. INTRODUCTION

It is now understood that at asymptotically large densities, the ground state of 3-flavor, massless QCD is the Color-Flavor Locked (CFL) configuration [1–3]. In this phase, quarks of all three flavors near the (shared) Fermi surface undergo BCS-like pairing due to the attractive one gluon exchange potential. The resulting condensate breaks the $U(1)_B$ symmetry associated with conserved baryon number, and also breaks the original $SU(3)_{color} \times SU(3)_L \times SU(3)_R$ symmetry down to the diagonal subgroup, $SU(3)_{C+L+R}$, causing the gauge bosons of the original $SU(3)_{color}$ group to become massive. However, a linear combination of the eighth gluon and the gauge boson of the $U(1)_Q$ symmetry (the photon) remains massless; this unbroken gauge symmetry will be referred to as $U(1)_{\tilde{Q}}$, denoting physically a “rotated” electromagnetism.

It was originally suggested that due to the large value of the gap the number densities of the three quark flavors would remain equal even when perturbations (non-zero quark masses and charge chemical potential) were included, since the energy cost of breaking pairs exceeded the energy gained by allowing the Fermi spheres for different flavors to relax past

^{*}abk4@u.washington.edu

[†]norsen@phys.washington.edu

one another [4,5]. It was soon realized, however, that there exists an energetically cheaper mechanism by which the CFL phase could relax under the influence of stresses: meson condensation [6,8]. For example, turning on a realistic mass for the strange quark encourages the system to reduce the strangeness density relative to the density of up- and down-type quarks. Kaon condensation allows the strangeness density to be decreased without the costly breaking of pairs in the CFL background.

The phase diagram for CFL + meson condensates was explored in detail in Ref. [9]. It was found there that the symmetric CFL phase was favored only when the chemical potential for electric charge satisfied $|\mu_Q| \lesssim 10MeV$ and the quark chemical potential was many orders of magnitude greater than that expected in neutron star cores. At realistic densities, the ground state at zero lepton chemical potential (μ_ν) involves a condensate of K^0 while at very high μ_ν it is the positively charged kaon K^+ which condenses. This ensures overall electric charge neutrality in the presence of a dense background of electrons.

At intermediate μ_ν it was found that a homogeneous mixed phase consisting of both K^0 and K^+ condensates was most effective in lowering the free energy. This mixture sits at a free energy saddle point in the hadronic sector configuration space, but this saddle point becomes a global minimum when one includes the free energy contribution of leptons and imposes local electric charge neutrality.

One may expect, however, that this homogeneous mixed phase could be unstable toward the formation of a heterogenous mixed phase in which the meson condensate rotates toward the K^0 condensed phase in certain regions of space, and toward the K^+ phase in others. This would violate the original assumption of *local* electric charge neutrality, since the K^+ regions would become positively charged and the K^0 regions would become negatively charged. This is allowed so long as the volume fractions of the two phases are such as to conserve charge globally. The question of stability is then the question of whether the cost associated with surface and Coulomb energies can be made less than the energy gained by allowing the meson fields to slide down from the saddle point to regions of lower potential.

This is the issue addressed in this paper, which is organized as follows. After a quick review of the chiral Lagrangian formalism used to describe mesonic excitations above the symmetric CFL ground state, we argue that the standard approach to studying possible mixed phases (involving some version of the thin wall approximation) will not be appropriate in this case. We then present the results of a small-fluctuation stability analysis of the homogeneous K^0/K^+ mixed phase to derive the dispersion relations for the low-lying excitations and discuss their implications to neutron star cooling and other possible phenomenological issues.

II. MESON CONDENSATION IN CFL MATTER

Because of the identity between the symmetry breaking pattern in the vacuum structure of QCD and the symmetry breaking pattern in the CFL phase at high density, it is appropriate to use the same chiral Lagrangian description one uses to parametrize small excitations about the QCD vacuum to parametrize small fluctuations about the $SU(3)$ -symmetric CFL phase.

These low energy excitations are parametrized by $\Sigma = e^{2i\pi/f_\pi + \eta'/f_A}$ and $B = e^{\beta/f_B}$ (with $\pi = \pi^a T^a$) where π_a 's are the pseudo-scalar octet of Goldstone bosons which arise from

the breaking of chiral symmetry and T_a 's are Gell-Mann matrices. η' and β are Goldstone bosons due to breaking of the $U(1)_A$ (assumed to be a valid symmetry of the theory at high density) and $U(1)_B$ symmetries, respectively. Under the original symmetry of $SU(3)_L \times SU(3)_R \times U(1)_B \times U(1)_A$ the Σ field transforms as $(3, \bar{3})_{0, -4}$.

The quark mass matrix $M = \text{diag}(m_u, m_d, m_s)$ induces mass differences between the members of the octet and transforms as $(3, \bar{3})_{0, 2}$. Due to $U(1)_A$ charges only even powers of M are present in the effective Lagrangian. To the leading order, only the combination $\tilde{M} = |M|M^{-1} = \text{diag}(m_d m_s, m_u m_s, m_u m_d)$ that transforms as $(\bar{3}, 3)_{0, 4}$ contributes to explicit mass terms via the operator $\text{Tr}\Sigma\tilde{M}$. The operator $X = -M^\dagger M/2\mu$ acts as a chemical potential for flavor symmetries [8]. Here μ represents the quark chemical potential. The leading order chiral Lagrangian for the octet is then:

$$\mathcal{L} = f_\pi^2 \left[\frac{1}{4} \text{Tr} \left(D_0 \Sigma D_0 \Sigma^\dagger - v^2 \text{Tr} \vec{\nabla} \Sigma \cdot \vec{\nabla} \Sigma \right) + \frac{a}{2} \text{Tr} \tilde{M} (\Sigma + \Sigma^\dagger) + \frac{b}{2} \text{Tr} Q \Sigma Q \Sigma^\dagger \right] \quad (1)$$

where $v^2 = 1/3$ is the (squared) in-medium meson velocity. The covariant derivative is given by

$$D_0 \Sigma = \partial_0 \Sigma - i[\tilde{\mu}, \Sigma] \quad (2)$$

where $\tilde{\mu} = \mu_Q Q + X$ and μ_Q is the chemical potential for electric charge and $Q = \text{diag}(2/3, -1/3, -1/3)$. The coefficient a has been computed in Ref. [6,7] and is given by $a = \frac{3\Delta^2}{\pi^2 f_\pi^2}$. The coefficient b , which accounts for charge-dependent differences in the meson masses, has been previously estimated by dimensional analysis to be of order $b \sim \frac{\alpha\Delta^2}{4\pi}$ where α is the fine structure constant corresponding to the unbroken $U(1)_{\tilde{Q}}$ in the CFL phase. [9,10] The parameter Δ denotes the value of the gap, which we will always approximate by $\Delta = 100 MeV$.

The free energy density arising from Eq.(1) relative to the free energy density of the symmetric CFL phase is:

$$\Omega = \frac{f_\pi^2}{4} \left[\text{Tr}[\tilde{\mu}, \Sigma][\tilde{\mu}, \Sigma^\dagger] + v^2 \text{Tr} \vec{\nabla} \Sigma \cdot \vec{\nabla} \Sigma - 2a \text{Tr} \tilde{M} (\Sigma + \Sigma^\dagger - 2) - b \text{Tr}[Q, \Sigma][Q, \Sigma^\dagger] \right] \quad (3)$$

where Σ is an $SU(3)$ matrix characterizing the direction of the condensate in internal space. As shown in Ref. [9] all stationary points of the free energy for spatially homogeneous configurations will satisfy the matrix equation

$$0 = \left[\tilde{\mu} \Sigma^\dagger \tilde{\mu} \Sigma - a \tilde{M} \Sigma - b Q \Sigma^\dagger Q \Sigma \right] - h.c. \quad (4)$$

This equation has two solutions corresponding to minima of Eq. (3). The first such minimum corresponds to a K^0 condensate and is parametrized by

$$\Sigma = \exp \left[i \theta_{K^0} \begin{pmatrix} 0 & 0 & 0 \\ 0 & 0 & 1 \\ 0 & 1 & 0 \end{pmatrix} \right] \quad (5)$$

where θ_{K^0} is given by

$$\cos \theta_{K^0} = \frac{M_{K^0}^2}{\tilde{\mu}_{K^0}^2}. \quad (6)$$

Where $M_{K^0}^2 = a(m_d + m_s)m_u$ and $\tilde{\mu}_{K^0}^2 = (m_s^2 - m_d^2)/2\mu$ [9]. (The minimum exists whenever this angle is real.) Similarly, there exists a local minimum of the free energy corresponding to a pure K^+ condensate:

$$\Sigma = \exp \left[i \theta_{K^+} \begin{pmatrix} 0 & 0 & 1 \\ 0 & 0 & 0 \\ 1 & 0 & 0 \end{pmatrix} \right] \quad (7)$$

where θ_{K^+} is given by

$$\cos \theta_{K^+} = \frac{M_{K^+}^2 - b}{\tilde{\mu}_{K^+}^2 - b} \quad (8)$$

where $M_{K^+}^2 = a(m_u + m_s)m_d$ and $\tilde{\mu}_{K^+}^2 = \mu_Q + (m_s^2 - m_u^2)/2\mu$ and again the solution only exists when θ_{K^+} is real.

Between the two minima just mentioned, there exists a free energy saddle point configuration involving a mixed condensate of K^0 and K^+ . Parameterizing the condensate by

$$\Sigma = \exp \left[i \theta_{SP} \begin{pmatrix} 0 & 0 & \sin \phi \\ 0 & 0 & \cos \phi \\ \sin \phi & \cos \phi & 0 \end{pmatrix} \right] \quad (9)$$

one finds a solution to Eq. (4) with angles satisfying:

$$\cos \theta_{SP} = \frac{M_{K^0}^2}{\tilde{\mu}_{K^0}^2} + \frac{\tilde{\mu}_{K^+}(\tilde{\mu}_{K^+} - \tilde{\mu}_{K^0})}{b\tilde{\mu}_{K^0}} \left[\left(\frac{M_{K^+}^2 - \tilde{\mu}_{K^+}^2}{\tilde{\mu}_{K^+}} \right) - \left(\frac{M_{K^0}^2 - \tilde{\mu}_{K^0}^2}{\tilde{\mu}_{K^0}} \right) \right] \quad (10)$$

and

$$\sin^2 \phi = \frac{\left(\frac{M_{K^0}^2}{\tilde{\mu}_{K^0}^2} - \cos \theta_{SP} \right)}{\left(1 - \frac{\tilde{\mu}_{K^+}}{\tilde{\mu}_{K^0}} \right) (1 - \cos \theta_{SP})} \quad (11)$$

where as usual the solution is only a stationary point of the free energy if the angles θ_{SP} and ϕ are real.

It was found in Ref. [9] that this saddle point configuration becomes the true minimum of the free energy when one includes leptonic contributions to the free energy and imposes local electric charge neutrality (*i.e.*, homogeneity) on the system. In practice, this means that for a given quark chemical potential μ and lepton chemical potential μ_ν , the chemical potential for electric charge is determined by the constraint that the electron number density equal the number density of K^+ in the meson condensate:

$$\frac{(\mu_\nu - \mu_Q)^3}{3\pi^2} = -\frac{\partial \Omega_{meson}}{\partial \mu_Q} \quad (12)$$

where Ω_{meson} is given by Eq. (3).

III. HETEROGENOUS MESON CONDENSATION

It is well-known that the imposition of local electric charge neutrality is often unwarranted, and may hide a lower-energy configuration in which overall charge neutrality results from the cancellation of charge among regions of non-zero local charge density [11]. If this occurs, the resulting crystalline mixed phase may dramatically affect both the equation of state and various transport properties of the neutron star [12].

It is natural to wonder whether the assumption of local charge neutrality mentioned in the previous section was overly restrictive. We begin our analysis of this question by assuming that an inhomogeneous mixed phase of K^0 and K^+ condensed regions is indeed favored, and studying the nature of the boundary layer between two adjacent regions. For now we ignore electrostatic energy contributions and Coulomb screening effects. Following the approach of Ref. [13] we consider a planar boundary and fix the condensates to point in the K^0 and K^+ directions at $\pm\infty$ respectively. We then implement a relaxation procedure which allows the fields to interpolate between the two fixed boundaries in a way that minimizes the total free energy of the surface. Pressure equilibrium across the boundary imposes a constraint which fixes the value of μ_Q . The resulting boundary profile, parametrized by the angles θ and ϕ of Eq. (9), for a quark chemical potential $\mu = 400MeV$ is shown in Fig. 1.

The notable feature is the large thickness of the energetically favored boundary. One can understand it by comparing the two terms contributing to the excess free energy of the boundary: the gradient terms associated with spatial changes in the field configurations, and the “bulk” terms which tally the cost of being away from a free energy minimum while one traverses the boundary. Since the height of the free energy barrier between the two minima is very small (of order 10^3MeV^4), a very thick boundary is required in order to make the two contributions comparable, and hence to minimize the overall surface tension. In the example shown, the surface tension turns out to be the quite small value $\sigma = 0.082MeV/fm^2$.

However, a boundary layer between K^0 and K^+ regions with thickness of several hundred fm is not allowed physically, since the Debye screening length of all charged species is much smaller than this length scale. Any structure of this enormous size would be warped out of existence as charge flowed in response to the large electric fields. We can estimate the role of screening by considering the energetics of a single charged droplet of the charged, lower-energy-density phase immersed in a background of the original phase. Ignoring for the moment the Coulomb contribution to the energy, we find

$$E(R) \sim \frac{4}{3}\pi\Delta\epsilon R^3 + 4\pi\sigma R^2 \quad (13)$$

where $\Delta\epsilon \leq 0$ is the bulk (free) energy density difference of the two phases. Any droplet larger than $R_{crit} \sim 3\sigma/|\Delta\epsilon|$ will be energetically favored compared to the homogeneous phase, and the volume and surface terms in the energy are of comparable size for droplets of radius near R_{crit} . In order for the droplet to be stable against charged particle flow (Debye screening), the Coulomb contribution to $E(R)$ must be a small correction to the terms already written. Estimating the Coulomb term by $E_C(R) \sim \alpha\rho_Q^2 R^5$ (where ρ_Q is the electric charge density of the droplet) then gives

$$\alpha \ll \frac{|\Delta\epsilon|^3}{\sigma^2\rho_Q^2} \quad (14)$$

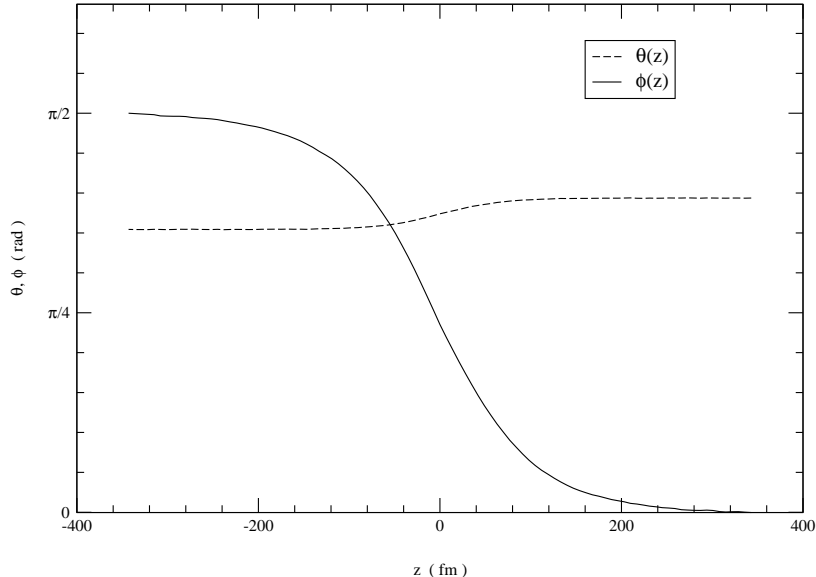


FIG. 1. Minimal-surface-tension boundary profile between regions of pure K^0 condensed matter and pure K^+ condensed matter at a quark chemical potential $\mu = 400MeV$. The bulk phases on either side of the boundary are at equal pressures. The effects of static Coulomb screening are here ignored. The surface tension found by integrating the excess free energy density across the boundary is $\sigma = 0.082MeV/fm^2$.

as the condition for the existence of a charge-separated mixed phase. In the present case, the right hand side is of order 10^{-8} and a stable heterogenous mixed phase (in which each phase sits at one of the local minima of the free energy density) is clearly ruled out for the physical value $\alpha \sim 1/137$.

If a heterogenous mixed phase is formed, then, it will have to involve only smaller departures from the homogeneous saddle point configuration. The condensate may “slide down” toward the K^0 configuration in one region of space, and similarly “slide down” toward the K^+ configuration in an adjacent region, but it cannot slide all the way down to the free energy local minimum. And without any definite guess as to the bulk field configurations in each region, it is difficult to study the energetic favorability of possible mixed phases in the standard way – that is, by taking an ansatz for the mixed phase configuration, treating the boundary as “thin”, varying with respect to appropriate parameters (droplet size, *etc.*), and comparing the total free energy to the free energy of the homogeneous phase.

We therefore take a somewhat different approach and study the stability of small perturbations to the homogeneous saddle point configuration. Any unstable modes will signal the instability of the homogeneous phase toward the production of some (largely unspecified) heterogenous mixed phase.

We present the full results of our analysis of the excitation spectrum in the next section; here we will simply quote those results which are relevant to the question of the stability of the homogeneous mixed phase. As we show in detail in Sec. IV the kaonic excitations about the homogeneous, charge neutral configuration consist of two massive kaons, one massless Goldstone boson arising from the breaking of $U(1)_Y$, and a massive in-medium longitudinal photon (which acquired a mass through the Higgs mechanism by eating one of the kaonic degrees of freedom). Plane-wave oscillations of this longitudinal photon degree of

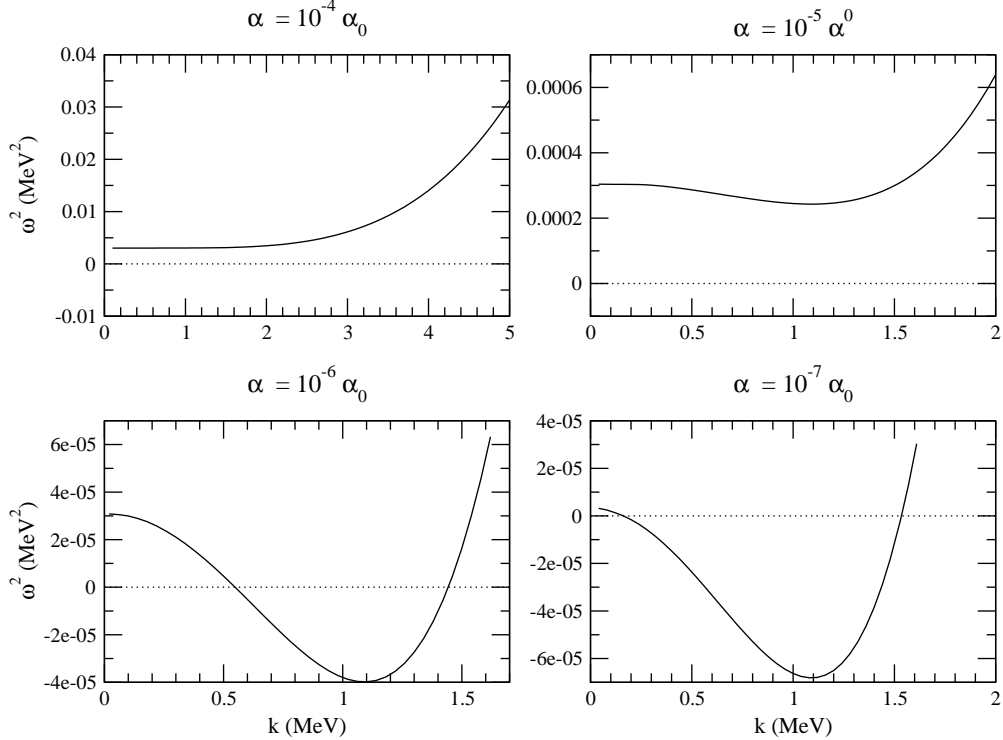


FIG. 2. Dispersion curves for the longitudinal photon mode for several values of α . (α_0 represents the value $1/137$.) The quark chemical potential is set to $\mu = 400\text{MeV}$ while $\mu_\nu = 100\text{MeV}$. For $\alpha \leq 10^{-6}\alpha_0$ the energy of the mode becomes pure imaginary (for a certain range of wavelengths), corresponding to an instability. Debye screening by electrons is included by giving the longitudinal photon an additional mass squared term equal to $k_D^2 = q^2\mu_e^2/(2\pi^2)$. Note also that the Higgs contribution to the photon mass is proportional to the electric charge q ; hence the overall reduction in scale as α is reduced.

freedom represent longitudinal charge density waves – just the sort of excitations which will be unstable if the homogeneous phase can lower its energy by forming a charge-separated mixed phase.

In Fig. 2 we show the dispersion relation for this mode as the electric charge α is varied. The longitudinal charge density wave is clearly a stable, massive mode until α is reduced many orders of magnitude below the physical value. Note that the critical value of α is not too far from the naive estimate made above based on consideration of macroscopic droplet properties. Also, the static plasma wave is most unstable for wave vectors $|\mathbf{k}| \sim 1\text{MeV}$ which corresponds to charged structures with a size of $D \sim 1/|\mathbf{k}| \sim 200\text{fm}$. This is again comparable to the size expected from the minimal-surface-tension boundary constructed above and shown in Fig. 1 – and is safely smaller than the charged particle Debye screening lengths for such tiny α . We conclude that in real high density matter where $\alpha \sim 1/137$ the homogeneous K^+/K^0 mixed phase is indeed stable against the production of a heterogenous, charge-separated configuration. The energetic cost of Coulomb and surface/gradient energy wins out over the energy savings associated with lowering the bulk energy densities.

IV. EXCITATION SPECTRUM

Having established that the homogeneous K^+/K^0 mixed is indeed the true ground state of matter at high density and nonzero neutrino chemical potential, we are now interested in finding the normal modes and dispersion relations for excitations above the ground state. The homogeneous background condensate is given by

$$\Sigma_0 = \exp \left[i \theta_{SP} \begin{pmatrix} 0 & 0 & \sin\phi \\ 0 & 0 & \cos\phi \\ \sin\phi & \cos\phi & 0 \end{pmatrix} \right] \quad (15)$$

where the angles are given by Equations (10) and (11). In order to parameterize small fluctuations about this state, we write the condensate as

$$\Sigma = \xi_0 \hat{\Sigma} \xi_0 \quad (16)$$

where $\xi_0 = \Sigma_0^{1/2}$ and

$$\hat{\Sigma} = \exp(2i\hat{\pi}/f_\pi). \quad (17)$$

Here $\hat{\pi} = \hat{\pi}_a T_a$ characterizes small rotations away from the homogeneous saddle point configuration given by Σ_0 .¹

In order to account for the Coulomb energy associated with possible charge separation, we must include the coupling of our meson fields to the gauge field associated with the unbroken $U(1)_{\tilde{Q}}$. This is accomplished by promoting the electric charge chemical potential to the role of a space- and time-dependent field. (For the following analysis, we will work in the Coulomb gauge $\vec{\nabla} \cdot \mathbf{A} = 0$ in which, to quadratic order in the Lagrangian, the transverse photon modes decouple from the hadronic excitations. Hence for our purposes we only need to keep track of the electrostatic potential. The transverse photon modes will acquire a mass via the Higgs mechanism in the standard way.) In particular, since we are concerned only with small perturbations about the homogeneous phase, we replace

$$\mu_Q \rightarrow \mu_Q + \delta A_0(\mathbf{x}, t) \quad (18)$$

where μ_Q is the constant value found by requiring the homogeneous phase to be electrically neutral, and δA_0 characterizes local fluctuations in the electrostatic potential. Note that from now on, we ignore the distinction between Q and \tilde{Q} charges. This is expected to be physically accurate for accessible densities, where the mixing angle between the new and old electromagnetism is small [15].

Substituting Equations (16) and (18) into our Lagrangian, and keeping only terms bilinear in fields we arrive at:

¹This helpful parameterization was suggested by David Kaplan.

$$\begin{aligned}
\mathcal{L} = & \text{Tr} \left(\partial_t \hat{\pi} \partial_t \hat{\pi} - v^2 (\vec{\nabla} \hat{\pi})^2 \right) - i \text{Tr} \partial_t \hat{\pi} ([\mu_R, \hat{\pi}] + [\mu_L, \hat{\pi}]) \\
& + f_\pi q \delta A_0 \text{Tr} \partial_t \hat{\pi} (Q_R - Q_L) - i f_\pi q \delta A_0 \text{Tr} ([Q_R, \mu_L] - [Q_L, \mu_R]) \hat{\pi} \\
& - \frac{1}{2} f_\pi^2 q^2 \delta A_0^2 \text{Tr} (Q_R Q_L - Q^2) - \text{Tr} [\mu_L, \hat{\pi}] [\mu_R, \hat{\pi}] \\
& - a \text{Tr} (M_L + M_R) \hat{\pi}^2 + b \text{Tr} [Q_L, \hat{\pi}] [Q_R, \hat{\pi}] \\
& + \frac{1}{2} (\vec{\nabla} \delta A_0)^2 - \frac{1}{2} \delta A_0^2 \Pi_{elec}^{00}(\omega, k)
\end{aligned} \tag{19}$$

where we have defined:

$$\begin{aligned}
\mu_R &= \xi_0 \tilde{\mu} \xi_0^\dagger \\
\mu_L &= \xi_0^\dagger \tilde{\mu} \xi_0
\end{aligned} \tag{20}$$

$$\begin{aligned}
M_R &= \xi_0^\dagger \tilde{M} \xi_0^\dagger \\
M_L &= \xi_0 \tilde{M} \xi_0
\end{aligned} \tag{21}$$

$$\begin{aligned}
Q_R &= \xi_0 Q \xi_0^\dagger \\
Q_L &= \xi_0^\dagger Q \xi_0.
\end{aligned} \tag{22}$$

(Note that the definitions of M_R and M_L differ from the other two cases.) In the last line of Eq. (19) the first term represents the electrostatic field energy, while the second accounts for the coupling of the background electron bath to the electric potential.

The factor $\Pi_{elec}^{00}(\omega, \mathbf{k})$ is the contribution to the temporal photon mass (squared) arising from the background electron gas. The leading-order (gauge-invariant) contribution to this quantity can be written down exactly for the case of a degenerate, relativistic electron gas [16,17]. It is:

$$\Pi_{elec}^{00}(\omega, \mathbf{k}) = k_D^2 \left(\frac{\omega}{2|\mathbf{k}|} \ln \left| \frac{\omega + |\mathbf{k}|}{\omega - |\mathbf{k}|} \right| - 1 \right) \tag{23}$$

where $k_D^2 = \frac{q^2 \mu^2}{2\pi^2}$ is the (squared) electron Debye screening length. We have omitted a possible imaginary part which describes Landau damping. We expect this damping to become important only for $|\mathbf{k}| \sim \mu_e$. Note that in the static limit $\omega \ll |\mathbf{k}|$ the electron Debye contribution to the photon mass squared becomes simply the constant k_D^2 . This was the approximation used in the previous section when studying the stability of the homogeneous configuration. In the present section, we retain the full expression. The effect of the electrons for $|\mathbf{k}| \lesssim k_D$, it turns out, is merely to increase the effective mass of the temporal photon by $1 - 2MeV$ above the mass it gets via the Higgs mechanism.

It is now possible to use symmetries to determine the superselection rules, and make a separate (sparse) ansatz for $\hat{\pi}$ for each non-interacting group of excitations. The simplest such group is the charged pions, π^+ and π^- . We will show the details of this calculation for pedagogical purposes and omit them in the physically more interesting case of kaonic excitations, which we treat next. Writing the pion fields in terms of their real and imaginary parts we have:

$$\hat{\pi} = \frac{1}{\sqrt{2}} (\pi_1 T_1 + \pi_2 T_2) \tag{24}$$

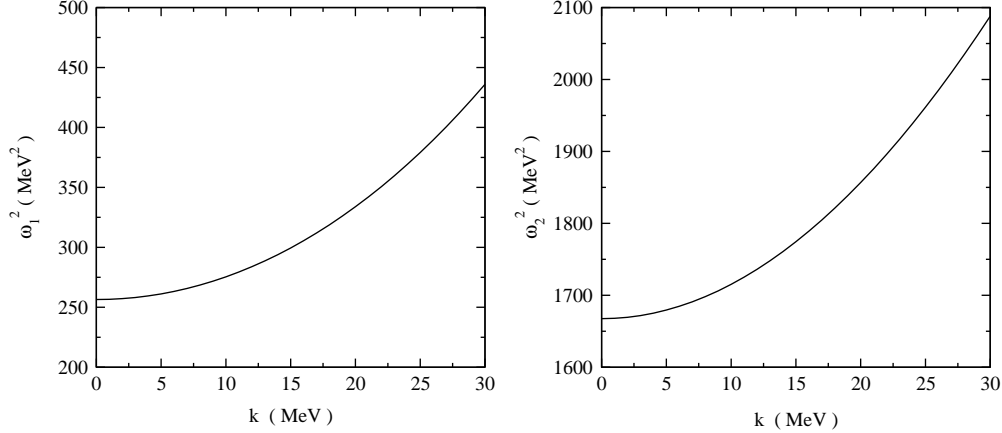


FIG. 3. Dispersion curves for the two charged pion normal modes at $\mu = 400\text{MeV}$ and $\mu_\nu = 100\text{MeV}$. The first normal mode corresponds to an almost pure π^- state with a numerically tiny admixture of π^+ ; *vice versa* for the second mode. The in-medium masses of the two charged pions are approximately 15MeV (for the π^- -like state) and 40MeV (for the π^+ -like state). The large mass splitting between the differently charged states arises from the nonzero value of the charge chemical potential, μ_Q .

where T_a are $SU(3)$ generators with $\text{Tr}(T_a T_b) = (1/2)\delta_{ab}$. Inserting Eq. (24) into the Lagrangian Eq. (19) and taking appropriate derivatives yields three coupled Euler-Lagrange equations for the fields π_1^\pm , π_2^\pm , and δA_0 . Taking a plane wave ansatz for each field

$$\begin{pmatrix} \pi_1(\mathbf{x}, t) \\ \pi_2(\mathbf{x}, t) \\ \delta A_0(\mathbf{x}, t) \end{pmatrix} \rightarrow \begin{pmatrix} \pi_1 \\ \pi_2 \\ \delta A_0 \end{pmatrix} e^{i(\mathbf{k}\cdot\mathbf{x} - \omega t)} \quad (25)$$

then gives a homogeneous linear system in the three field amplitudes. The solutions of this system represent the normal modes and dispersion relations. Since there is no term in the Lagrangian that depends on $\partial\delta A_0/\partial t$, the equation of motion for δA_0 – Poisson’s equation – should be interpreted as a constraint. (We are working in Coulomb gauge, where this is standard.) Hence, the system of three linearized equations of motion will have only two normal modes. The dispersion curves for these two modes (which are almost pure π^- and π^+ respectively) are shown in Fig. 3.

Because we are expanding about a background condensate consisting of both K^0 and K^+ , the neutral kaonic excitations may mix with the charged kaons. In order to find the normal modes and dispersion relations, we proceed as before, writing

$$\hat{\pi} = \frac{1}{\sqrt{2}} \left(K_1^0 T_6 + K_2^0 T_7 + K_1 T_4 + K_2 T_5 \right) \quad (26)$$

and substituting this ansatz into the quadratic Lagrangian. Requiring harmonic dependence on x and t as before gives a coupled system of five equations of motion for the field amplitudes. The dispersion relations for the four normal modes are shown in Fig. 4.

There is one exactly massless mode which can be identified as the Goldstone boson arising from the fact that the K^0/K^+ condensate breaks the $U(1)_Y$ hypercharge symmetry of the original theory. (Weak interactions, however, will give a small mass to this particle [18].)

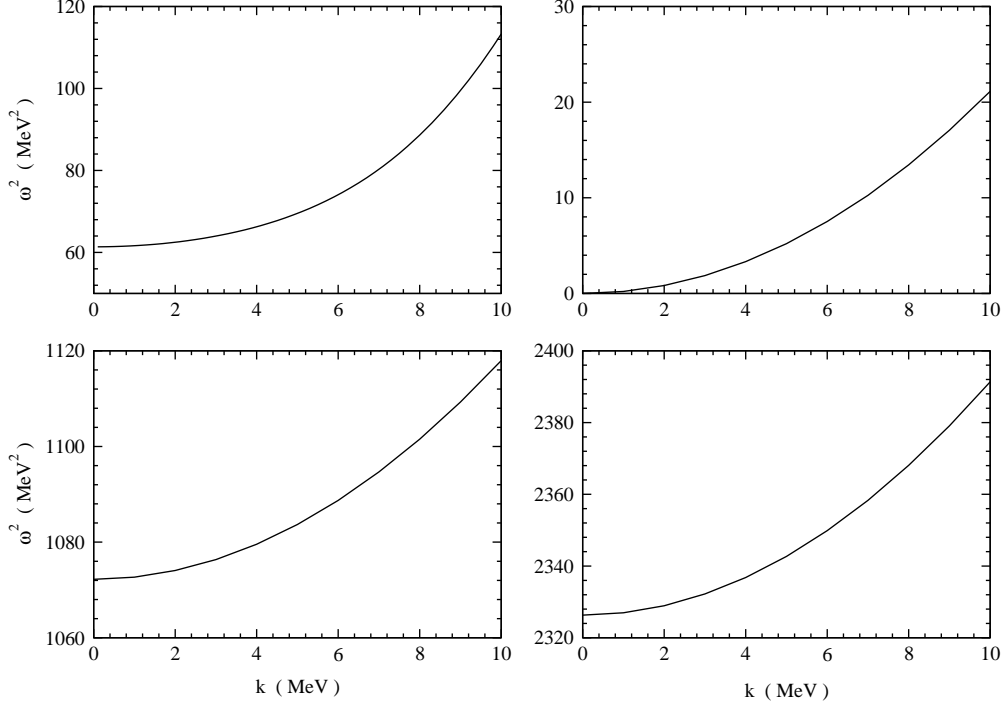


FIG. 4. Dispersion curves for the four kaonic normal modes at $\mu = 400\text{MeV}$ and $\mu_\nu = 100\text{MeV}$. The upper-left figure shows the longitudinal photon mode, which we have also described as a longitudinal plasma oscillation. With the physical value of the fine structure constant, this mode is stable ($\omega^2 > 0$) and the homogeneous K^0/K^+ mixed phase is the true ground state of the system. There are also two massive kaon modes, and a single massless mode arising from the breaking of the $U(1)_Y$ hypercharge symmetry by the K^0 portion of the condensate.

This Goldstone boson corresponds to K_2^0 in our above ansatz, *i.e.*, it consists of harmonic fluctuations in the imaginary part of the neutral kaon fields (as expected). There are also two massive modes (with masses of about 32MeV and 48MeV). The lighter of these is predominantly a K^0 with a small admixture of K_1^0 and K_1 , while the heavier is mostly a K^- with a small admixture of K^0 . Finally, the temporal photon mode (consisting, as expected, of the imaginary part of the charged kaon field plus a sizable electric field) weighs in with a mass of about 8MeV . As discussed previously, this mode (which came from the photon eating the would-be-Goldstone-boson from the breaking of $U(1)_{\tilde{Q}}$) corresponds physically to a plane-wave plasma oscillation of the (rotated) electric charge density. Note again that the background condensate breaks the usual superselection rules and allows the excitations to be coherent mixtures of states with different hypercharges and (rotated) electric charges.

V. DISCUSSION

We have shown that the homogeneous K^0/K^+ condensate in CFL matter at non-zero μ_ν is stable against the production of a heterogenous, charge-separated mixed phase. Due to the very short potential energy barrier between the pure K^0 and K^+ phases, the cost of surface and Coulomb energies is too large for charge separation to be energetically favorable. Although we have focussed our discussion on a single point in the μ - μ_ν phase diagram, the

stability of the homogeneous phase persists throughout the *CFL* K^0/K^+ region identified as the ground state in Ref. [9]. (As pointed out in Ref. [19], the Coleman-Weinberg mechanism [20] may produce a small additional incentive favoring the production of charge-separated domains. However, this incentive appears to be either absent or negligible for realistic densities relevant to neutron star cores.)

The normal modes and excitation spectra we discussed in the previous section may be relevant for future calculations of the neutrino scattering rates in the cooling neutron star. Of special importance in this context is the relatively light ($m_\gamma \lesssim 10\text{MeV}$) photon mode. Since this excitation involves a spatially fluctuating density of electrons and charged and neutral kaons, one may expect large cross sections for neutrino scattering. The physics here is similar to that discussed in Ref. [21] where it is shown that coherent neutrino scattering from droplets of kaonic matter (whose weak charge density differs significantly from the hadronic background) will dramatically affect neutrino scattering rates and hence potentially observable neutrino light curves from supernovae. Equivalently in our problem, one expects that due to the spatial oscillation of the electron and kaon densities, the cross section for neutrino - photon scattering will be large and that the copious presence of such excitations for $T \gtrsim m_\gamma \sim 8\text{MeV}$ may significantly increase the time required for neutrinos to diffuse out of the proto-neutron star. One might hypothesize that only the relatively early-time neutrino light curve would be thereby stretched out in time since, if the dominant contribution to neutrino scattering rates indeed comes from these longitudinal photon excitations, there will be a relatively sudden change in the density of “targets” as the core temperature drops below m_γ .

Also, as discussed in Ref. [22], the breaking of various $U(1)$ symmetries (hypercharge and rotated electromagnetism) by the mixed kaon condensate will allow for the presence of global and/or gauged vortices and vortons. The present work, in determining the in-medium masses for the various kaonic excitations, thereby also fixes certain properties of kaonic vortices, *e.g.*, the distance scale over which a superconducting K^+ condensate at the center of a K^0 vortex will fall off with distance. The in-medium masses of the various components of the (rotated) photon will also be relevant for a detailed description of the spatial dependence of the electric and magnetic fields surrounding such vortices. These vortices may also affect the cooling history of young neutron star through their neutrino opacities and magnetic properties.

A more detailed treatment of the various particle-like and topological excitations above the homogeneous K^0/K^+ condensate, and especially their effects on neutrino scattering and diffusion, will be left for future work.

Acknowledgements

We thank David Kaplan, Guy Moore, and Sanjay Reddy for proposing this problem to us, and for many helpful discussions along the way. The work is supported in part by the US Department of Energy grant DE-FG03-00ER41132.

REFERENCES

- [1] M.G. Alford, K. Rajagopal, and F. Wilczek, Phys. Lett. **422B**, (1998) 247
- [2] R. Rapp, T. Schaefer, E.V. Shuryak, and M. Velkovsky, Phys. Rev. Lett. **81**, (1998) 53
- [3] D.T. Son, Phys. Rev. D **59**, (1999) 094019
- [4] K. Rajagopal and F. Wilczek, hep-ph/0012039
- [5] P. F. Bedaque, hep-ph/9910247
- [6] D.T. Son and M. A. Stephanov, Phys. Rev. D **61**, (2000) 074012 erratum, *ibid.* Phys. Rev. D **62**, (059902) 2000
- [7] S.R. Beane, P.F. Bedaque and M.J. Savage, Phys. Lett. **483B**, (2000) 131
- [8] P.F. Bedaque and T. Schaefer, hep-ph/0105150
- [9] D. Kaplan and S. Reddy, hep-ph/0107265
- [10] C. Manuel and M.H. Tytgat, Phys. Lett. **501B**, (2001) 200
- [11] N.K. Glendenning, Phys. Rev. D **46**, (1992) 1274
- [12] D.Q. Lamb, J.M. Lattimer, C.J. Pethick, and D.G. Ravenhall, Nucl. Phys. **A411**, (1983) 449
H. Heiselberg, C.J. Pethick, and E.F. Staubo, Phys. Rev. Lett. **70**, (1993) 1355
N.A. Gentile, M.B. Aufderheide, G.J. Mathews, F.D. Swesty, and G.M. Fuller, Astrophys. J. **414**, (1993) 701
A. Steiner, M. Prakash, and J.M. Lattimer nucl-th/0003066
N.K. Glendenning and J. Schaffner-Bielich, Phys. Rev. C **60**, (1999) 025803
- [13] M.B. Christiansen, N.K. Glendenning, and J. Schaffner-Bielich Phys. Rev. C **62**, (2000) 025804
- [14] T. Norsen and S. Reddy Phys. Rev. C **63**, (2001) 065804
- [15] M. Alford, K. Rajagopal, S. Reddy, F. Wilczek, hep-ph/0105009
- [16] C. Manuel, Phys. Rev. D **53**, (1996) 5866
- [17] E. Braaten, hep-ph/9303261
- [18] D. T. Son, hep-ph/0108260
- [19] P. F. Bedaque, nucl-th/0110049
- [20] S. Coleman and E. Weinberg, Phys. Rev. D **7**, (1973) 1888
- [21] S. Reddy, G. Bertsch, and M. Prakash Phys. Lett. **475B**, (2000) 1-8
- [22] D.B. Kaplan and S. Reddy, hep-ph/0109256